Establishing local TID climatology for Antarctic Peninsula region

V.V. Paznukhov[1], Y.M. Yampolski[2], V.G. Galushko[2], A.A. Sopin[2], and K.M. Groves[1]

[1] *Boston College, USA*
[2] *Institute of Radio Astronomy, Kharkov, Ukraine*

29 June 2016

2016 Beacon Satellite Symposium, Trieste, Italy

Outline

- Challenges of GNSS studies in Antarctica
- Interferometric methods
- TID study with GNSS TEC in Antarctica, 2009-2012
- Sensitivity of GNSS TEC (vs HF Observations)
- Summary

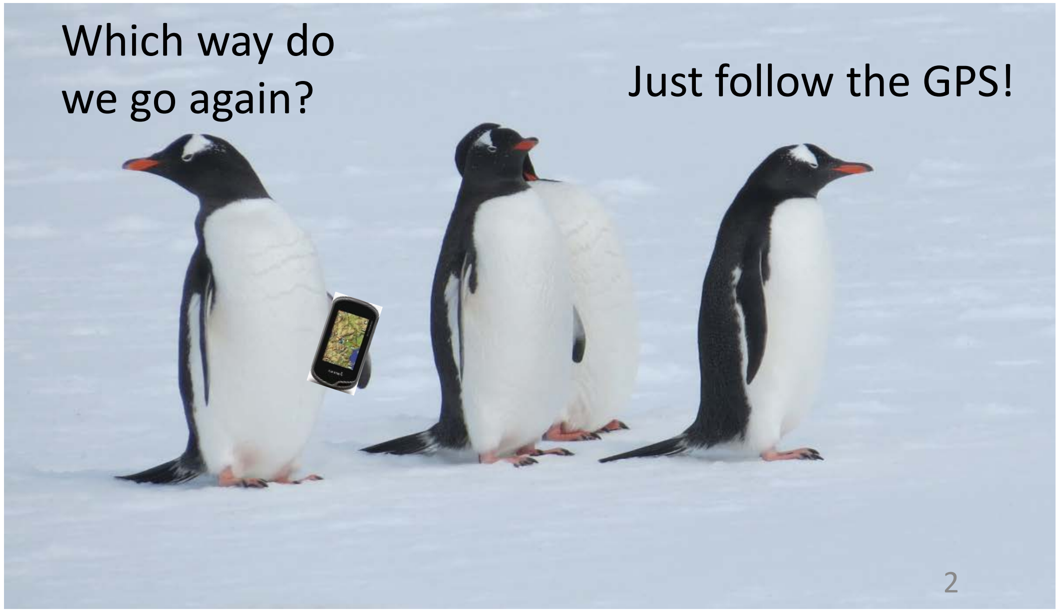

GPS TEC observations in Antarctic Peninsula region

Drake Passage in Antarctica generates severe tropospheric waves, i.e.,
It is associated with cyclones, convective plumes, enhanced zonal winds, orographic waves, etc.

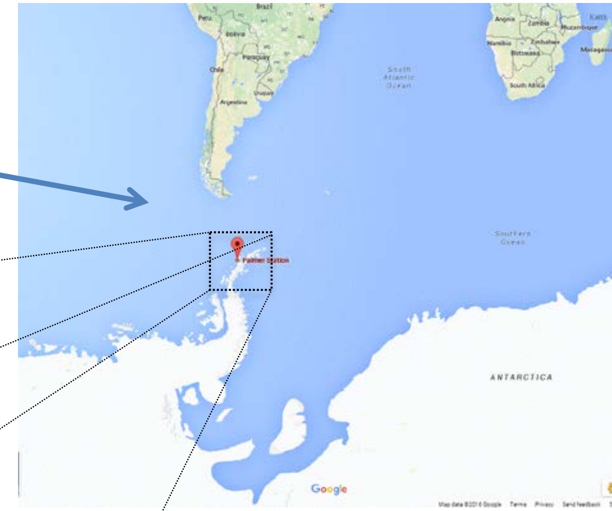

2009-2012

65 deg South geographically
~51 deg South geomagnetically

USA vs Antarctic Peninsula 1925 : 15

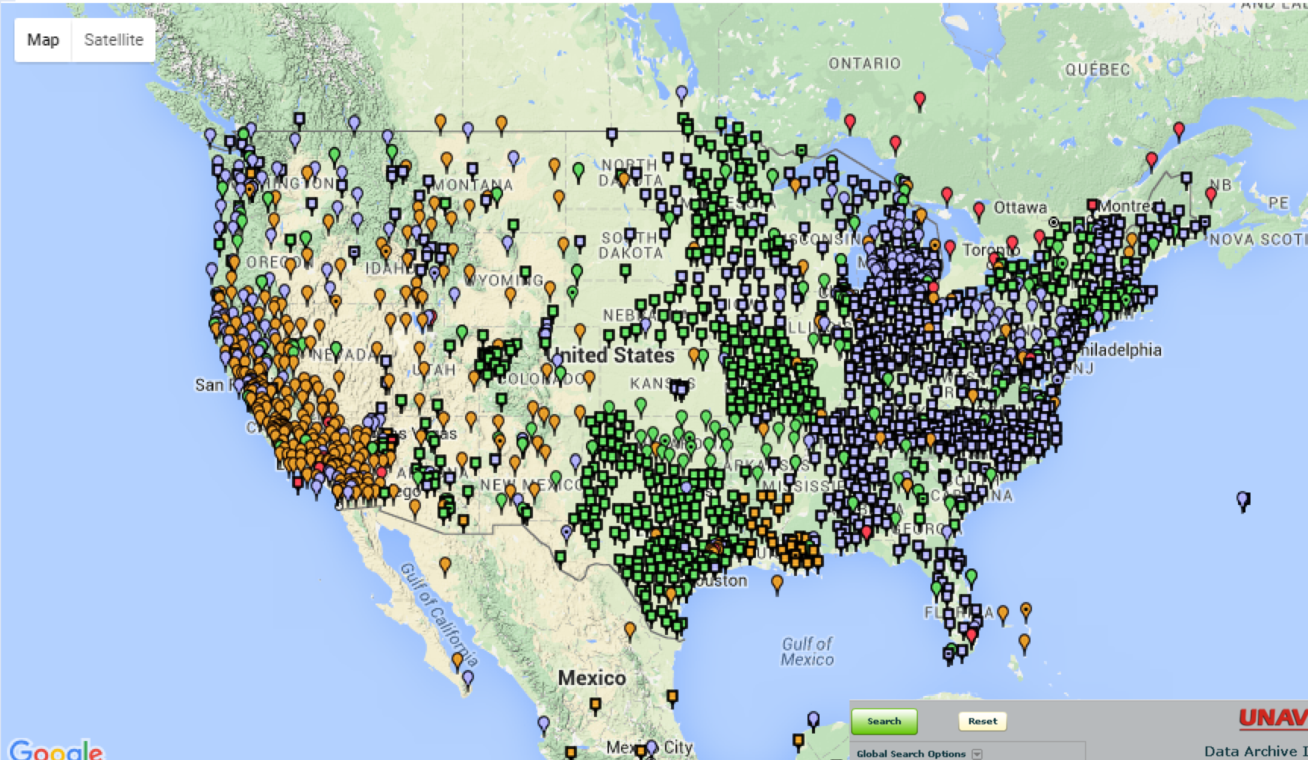

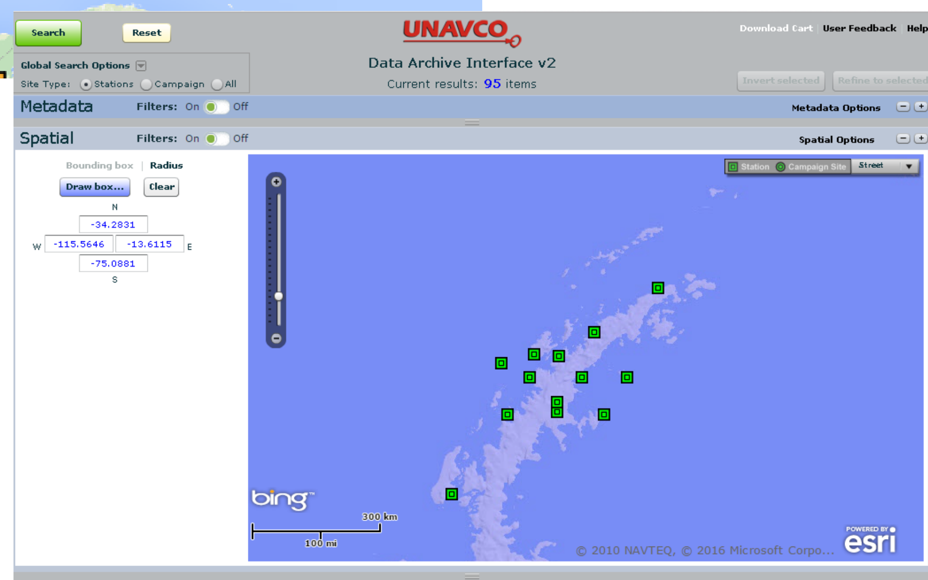

TEC maps for Antarctica?

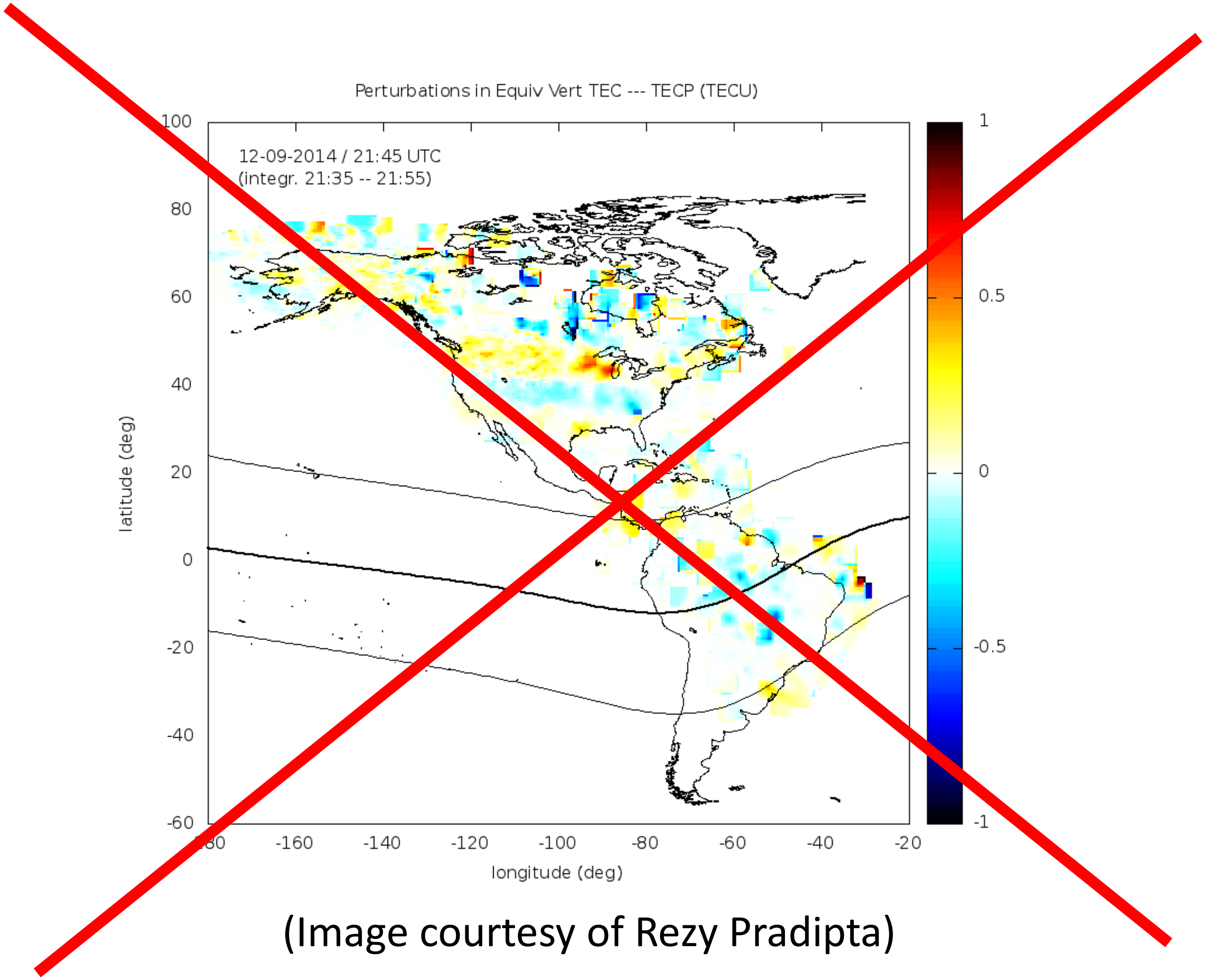

(Image courtesy of Rezy Pradipta)

GNSS interferometry methods

(Wan et al., 1997; Afraimovich et al., 1998; Hernandes-Pajares, 2006; Galushko et al., 2014 and others..)

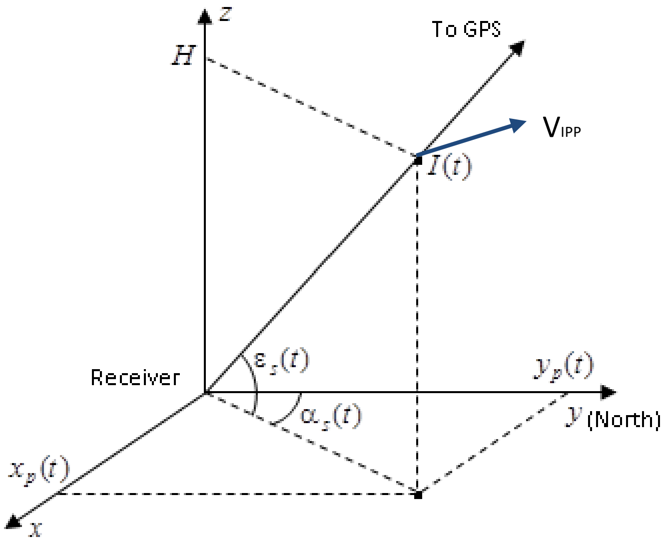

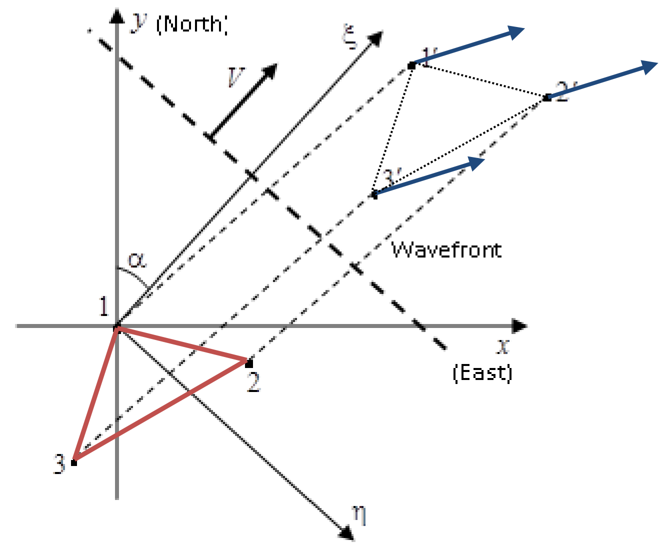

$$\omega' = \omega - k_x(\omega)V_{IPPx} - k_y(\omega)V_{IPPy} \Rightarrow \omega - \Delta\omega$$

TID GNSS Tests (Afraimovich method)

- Simulation of TID parameter derivation for a short 5-km baselines

Plane wave is assumed, e.g.,

$$\Delta\phi(t,x,y) = \delta \sin(\Omega t - K_x x - K_y y + \varphi_0)$$

(*TEC calculation by C. Carrano*)

E.L. Afraimovich et al./Journal of Atmospheric and Solar-Terrestrial Physics 60 (1998) 1205–1223

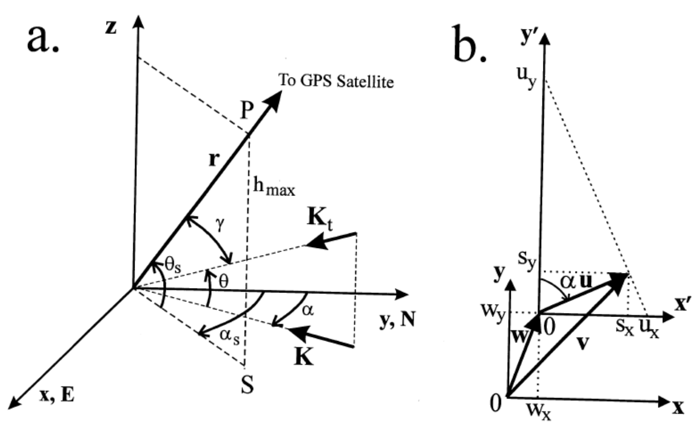

Then the phase differences $\Delta\phi$ between the receivers, spaced along the axes x and y, are proportional to the values of the horizontal components $G_x = I'_x$ and $G_y = I'_y$ of the TEC gradient; primes denote derivatives with respect to variables specified by a lower index. For convenience of presentation, we will be using values of phase as well as TEC. Phase differences $\Delta\phi$ are used to calculate its spatial derivatives $\phi'_x(t) = \Delta\phi/\Delta x$ and $\phi'_y(t) = \Delta\phi/\Delta y$ where Δx and Δy are distances between receivers spaced along the x and y axes.

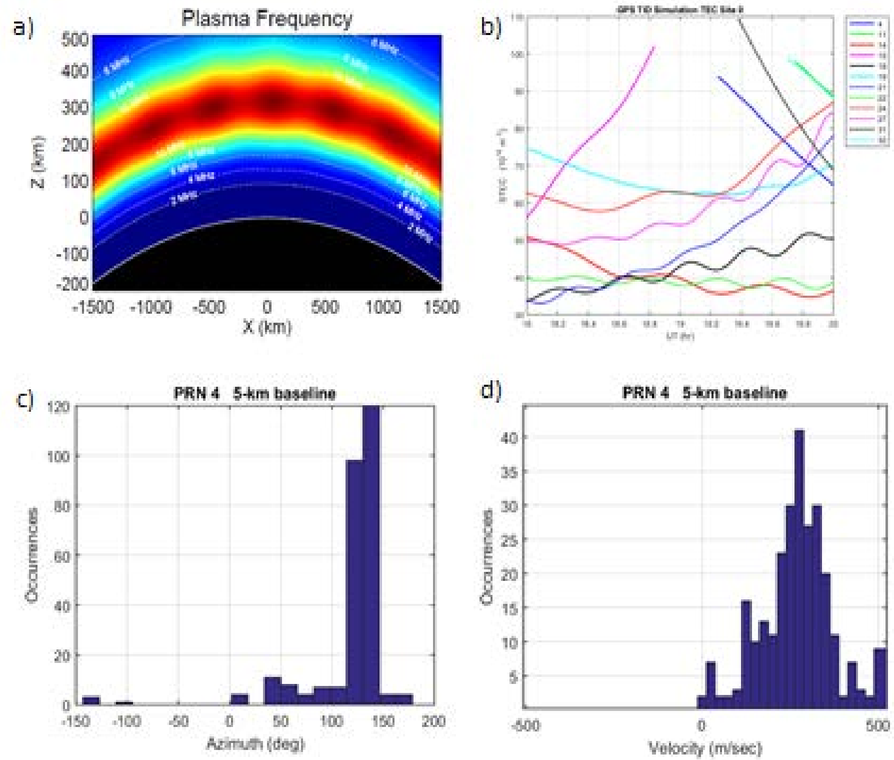

Interferometry for arbitrary shape of the disturbance

For any disturbance represented as $I(x,y,t) = I(x\sin\alpha + y\cos\alpha - Vt)$

[Galushko et al., 2016]

Solution is:

$$\sin\alpha(t) = \gamma_x(t) / \sqrt{\gamma_x^2(t) + \gamma_y^2(t)}$$

$$V(t) = \frac{1}{\gamma(t)}\left[\gamma_x(t)\frac{dx_p(t)}{dt} + \gamma_y(t)\frac{dy_p(t)}{dt} - I'(t)\right]$$

Where space and time derivatives are:

$$I'(t) = dI(x,y,t)/dt$$

$$\gamma_x(t) \equiv \partial I(x,y,t)/\partial x$$

$$\gamma_y(t) \equiv \partial I(x,y,t)/\partial y$$

Derivatives can be numerically calculated

$$I_1'(t_n) \approx \frac{I_1(t_n) - I_1(t_{n-1})}{\Delta t}$$

$$\gamma_x(t_n) \approx \frac{y_3 \cdot (I_2(t_n) - I_1(t_n)) - y_2 \cdot (I_3(t_n) - I_1(t_n))}{x_2 y_3 - x_3 y_2}$$

$$\gamma_y(t_n) \approx \frac{x_2 \cdot (I_3(t_n) - I_1(t_n)) - x_3 \cdot (I_2(t_n) - I_1(t_n))}{x_2 y_3 - x_3 y_2}$$

Data analysis constraints

Correlation coefficient between TECs from different stations:

$$K_{ij} \geq 0.5$$

To assure accuracy in azimuth calculation of better than 10 deg for the given GNSS station geometry it is necessary to satisfy:

$$|\gamma| \geq 15 \cdot 10^{-4} \quad \text{[TECu/km]}$$

Elevation angle > 30 deg

Data availability: April 2009 to June 2012

Data processing sequence

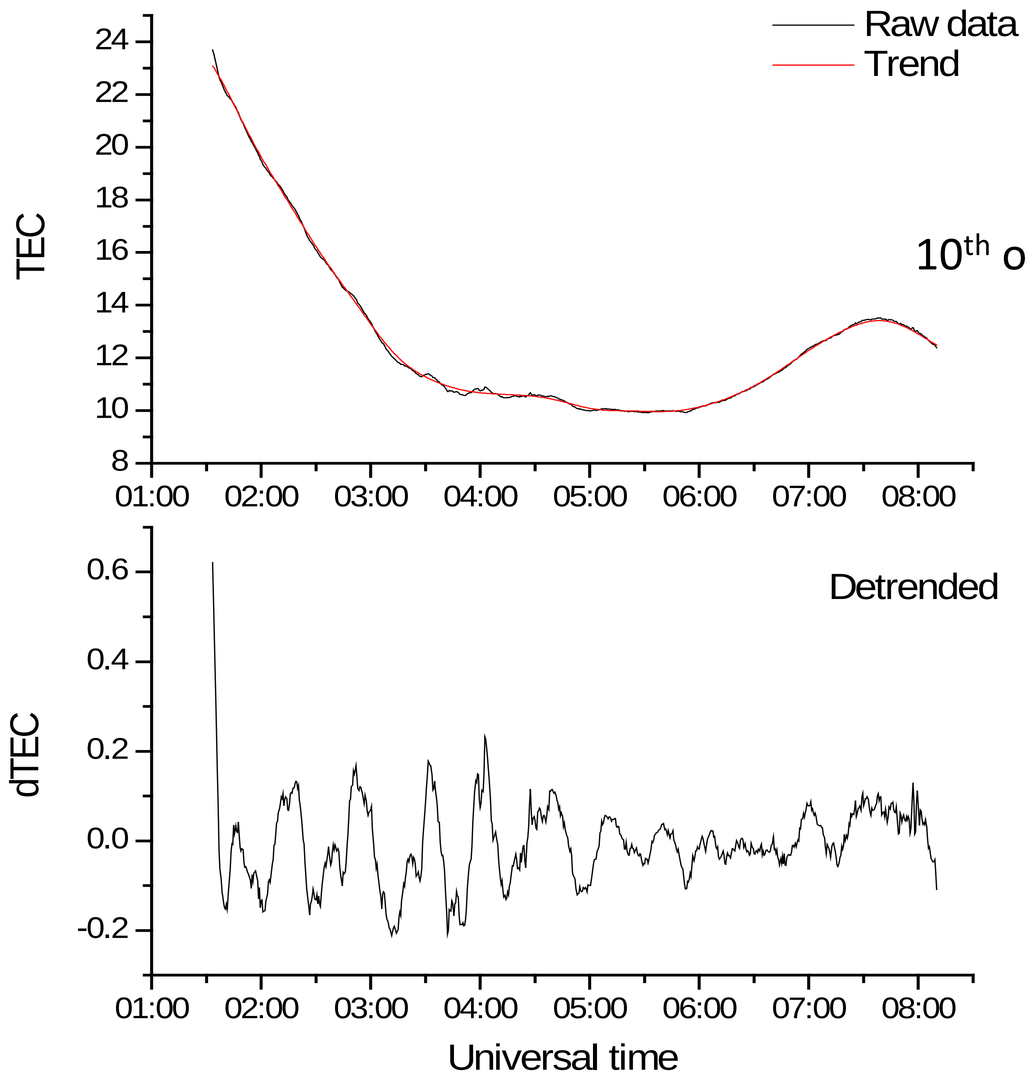

10th order polynomial

Detrended TEC data is smoothed with 5.5 min averaging window

Example of real preprocessed data

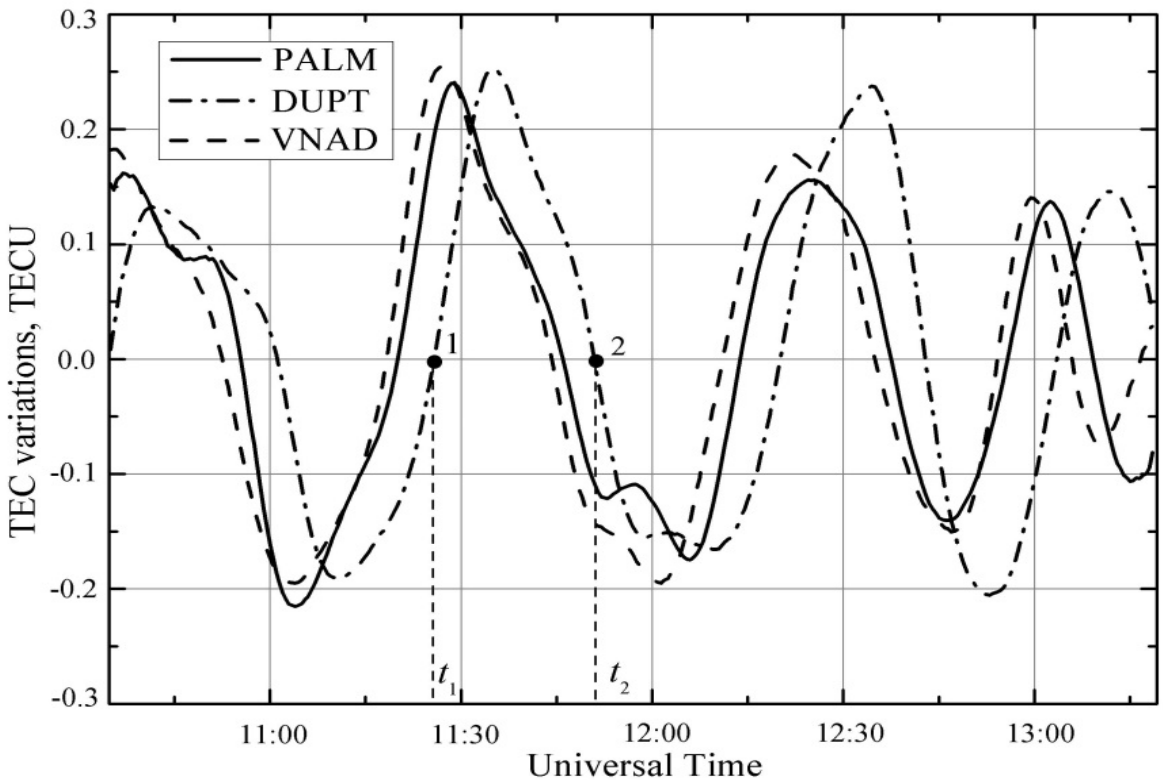

TEC records from three stations are well correlated.

$$K_{ij} \approx 0.8 - 0.9$$

Summer/Winter disturbances in Antarctica

[Galushko et al., 2016]

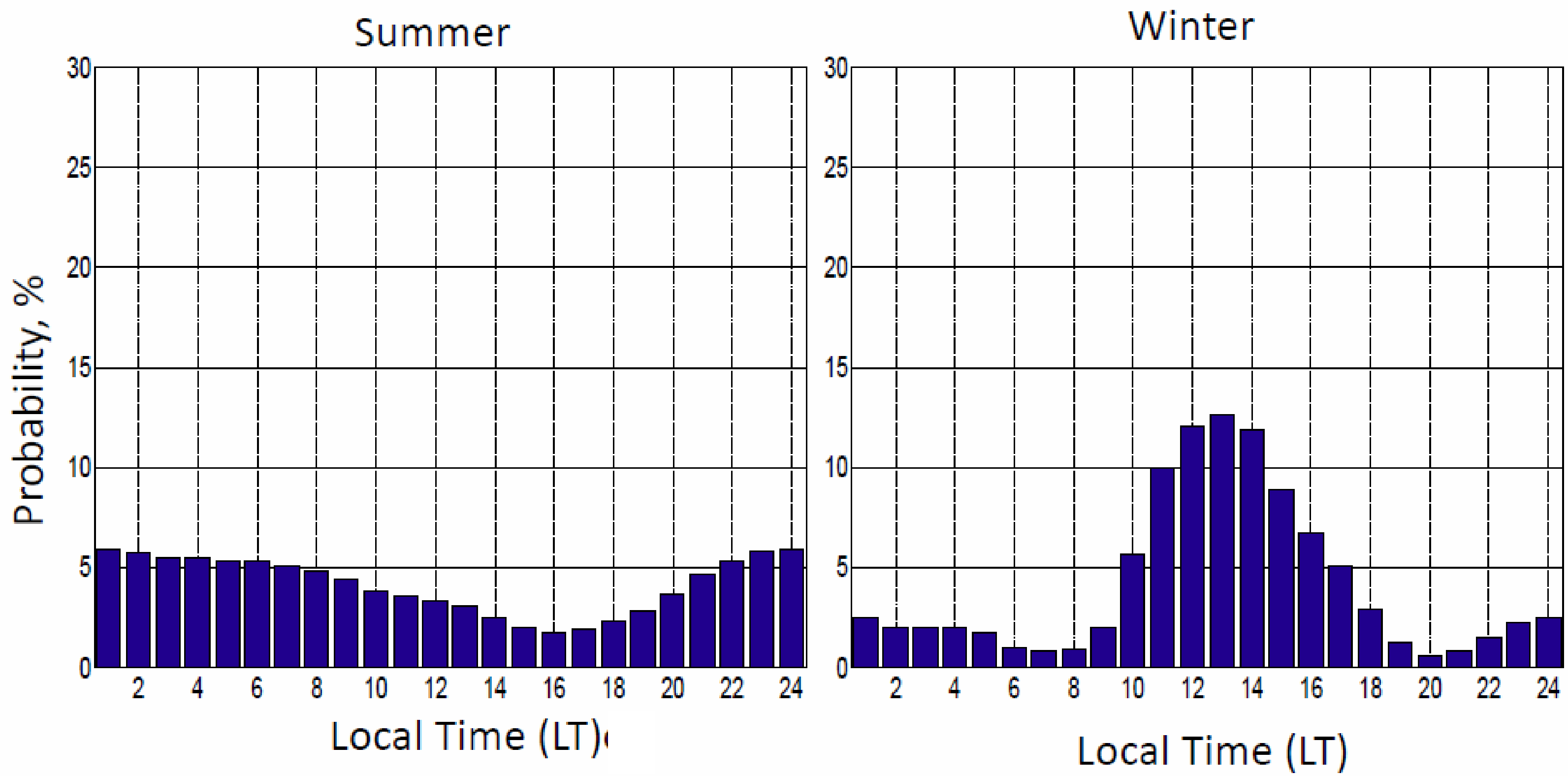

Summertime versus wintertime observations as functions of local time.
During the Antarctic winter time (Jun-Jul) disturbances are usually observed at local noon time, in sharp contrast with the summer, when disturbances are observed during the nights and mornings.

Observations during quiet/disturbed times I

[Galushko et al., 2016]

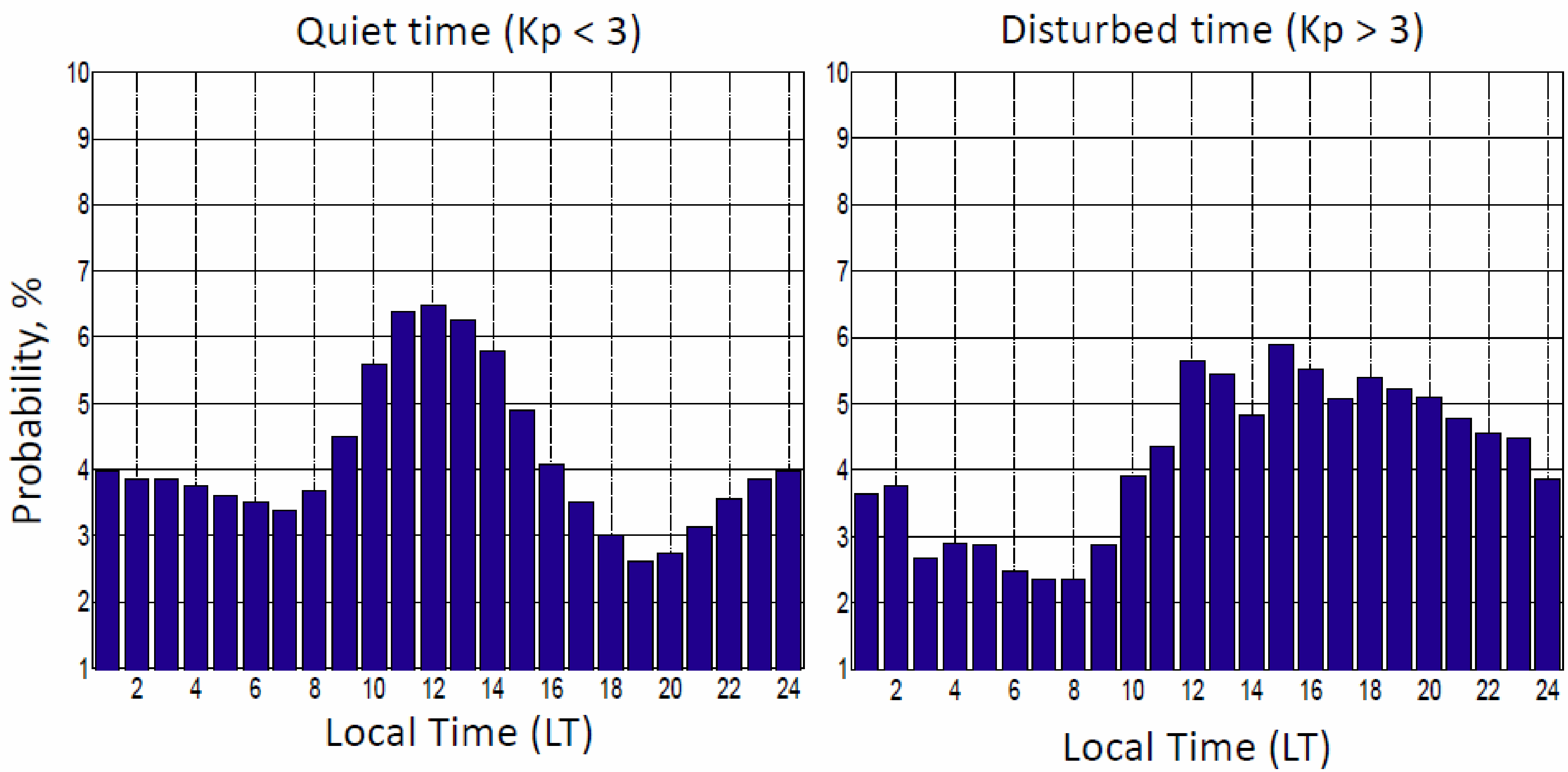

TID observations as a function of local time for quiet and disturbed periods. Quiet time events have a maximum near local noon time, while active time events are mainly observed in the afternoon and evening.

Observations during quiet/disturbed times II

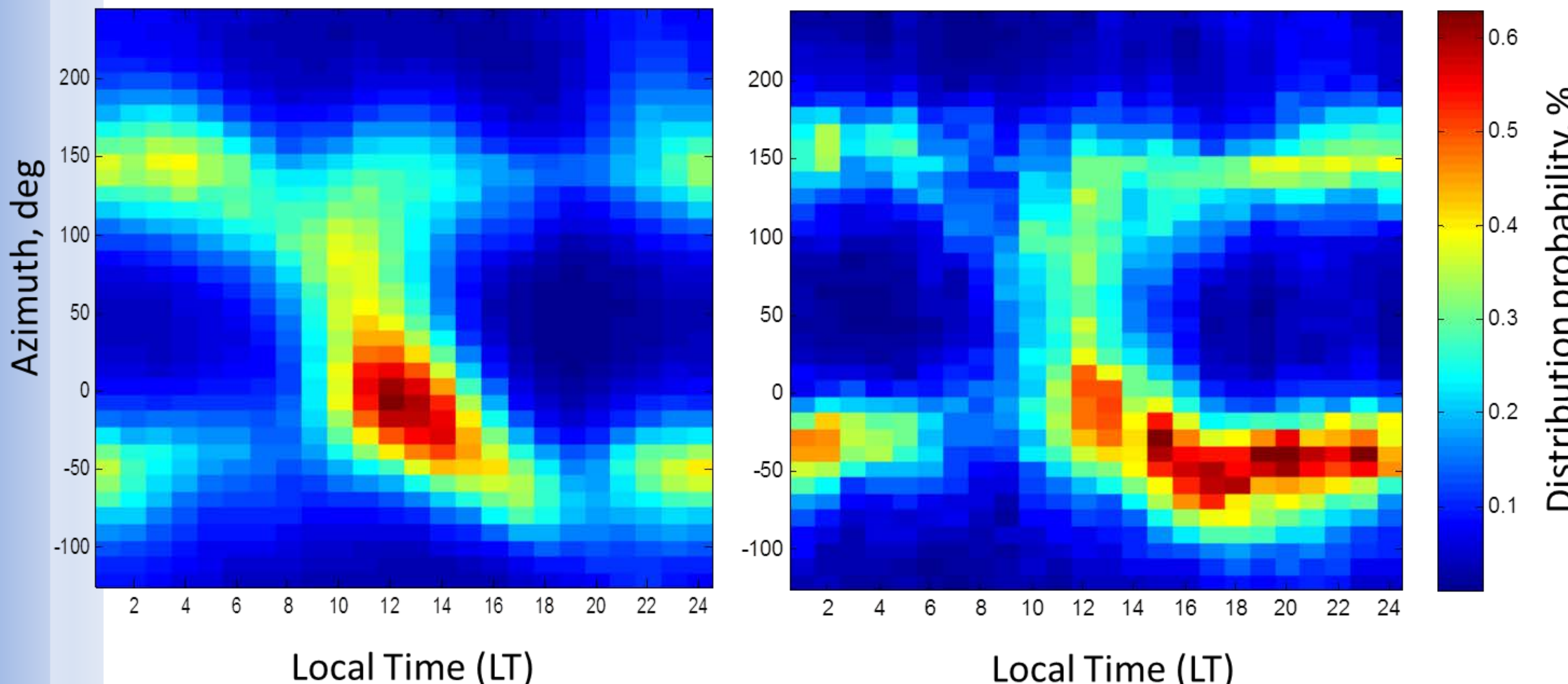

[Galushko et al., 2016]

Daily trends of TID direction (geographic azimuth) measured at Antarctic Peninsula during 2009-2012. Note that the disturbances observed during the disturbed periods predominantly propagate North and North-West, i.e., equatorward. Disturbances observed during the quiet time change azimuthal direction during the day, i.e., follow the anti-windward direction.

Velocity distribution

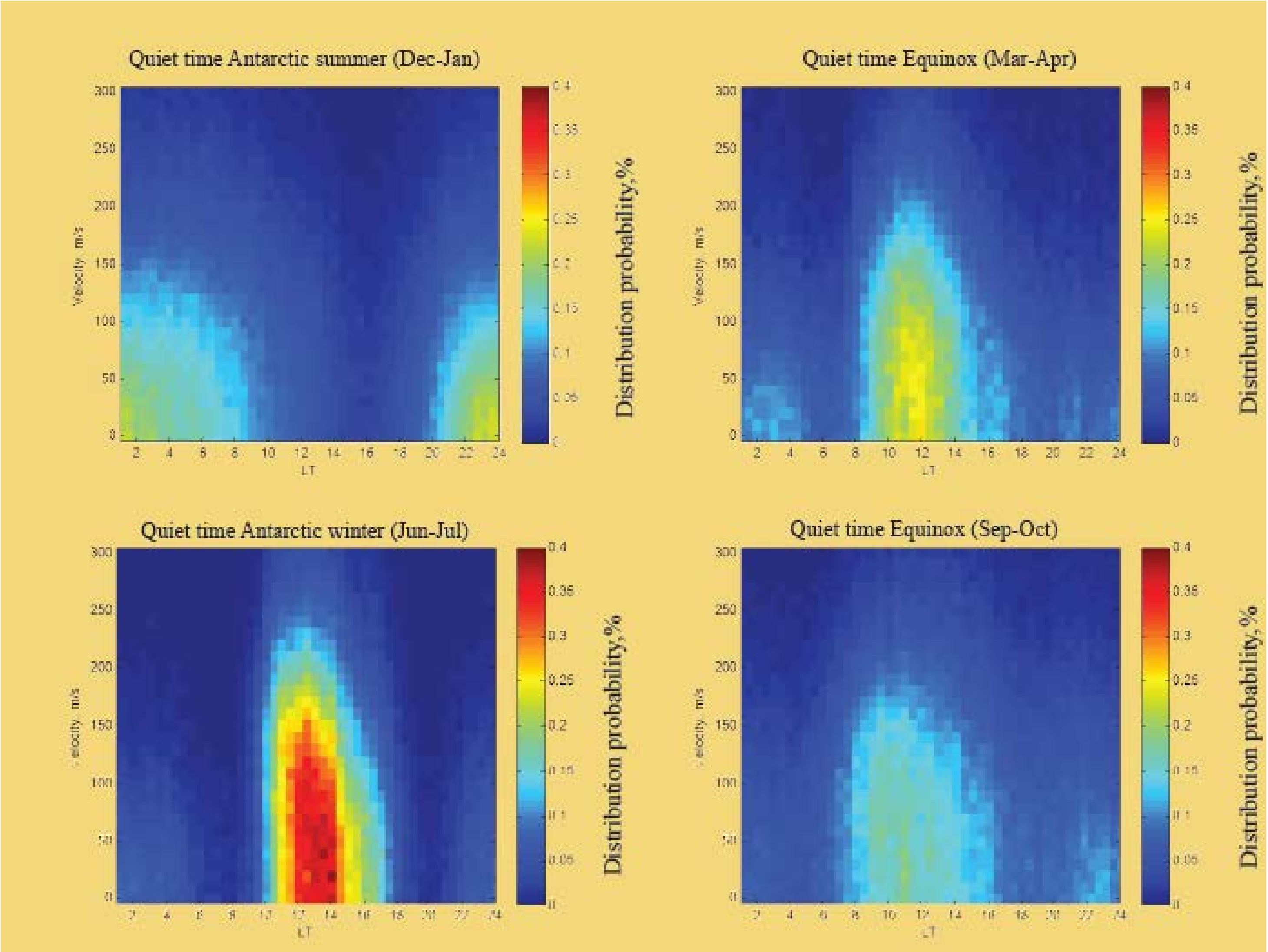

Velocity observations during four different seasons. During the summer time disturbances are characterized by lower velocities and tend to be observed in the morning and in the evenings. The highest velocities are observed during the winter time near noon time. Equinox time appear more similar to the winter.

Azimuthal distribution

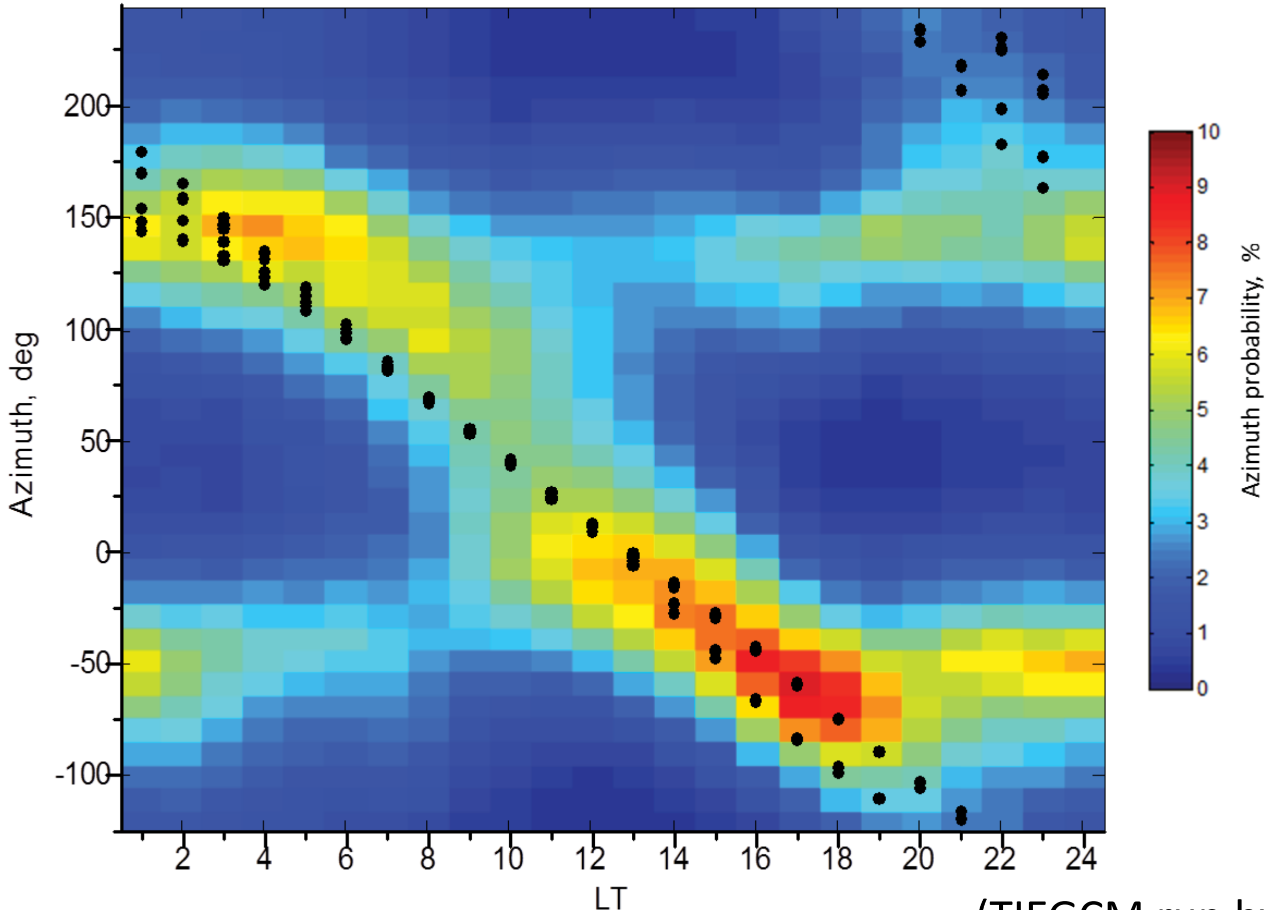

(TIEGCM run by Brett Carter)

"Perfect anti-match" between measured TID azimuth and modeled neutral wind direction (dots). The neutral wind is calculated with TIEGCM model for several quiet days in Jan-Apr 2011. In the figure the direction of the neutral wind is shifted by 180 deg, thus showing the "anti-windward" direction. Quiet-time TID measurements for the entire period of observations (2009-2012) are shown. Note that several TID modes are present simultaneously: one with changing azimuth and at least two others with constant azimuthal directions of about -50 deg and 150 deg.

Gravity waves tend to propagate in the anti-windward direction

The so-called wind filtering effect

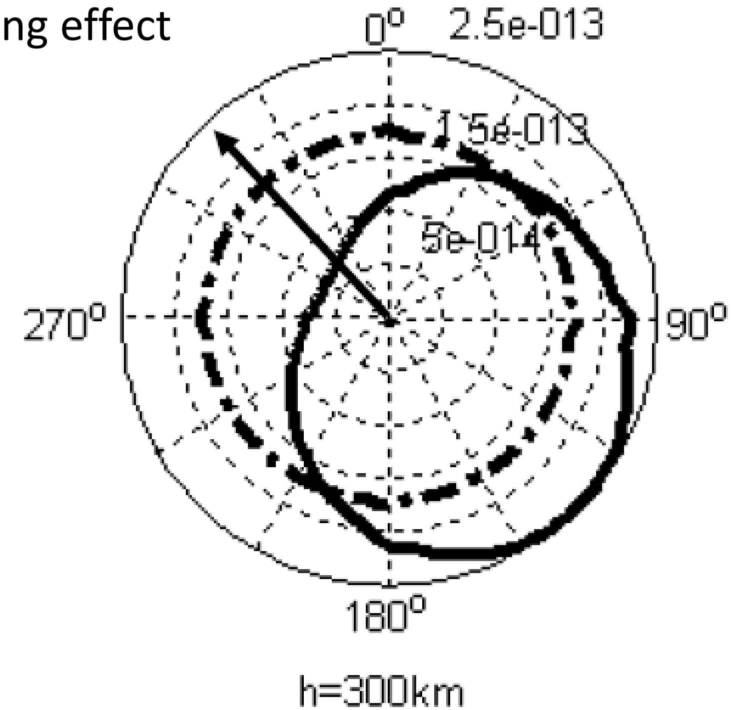

From: *Sun L., W. Wan, F. Ding, and T. Mao , Gravity wave propagation in the realistic atmosphere based on a three-dimensional transfer function model, Annales Geophysicae, Volume 25, Issue 9, 2007, pp.1979-1986*

Antarctic disturbance climatology

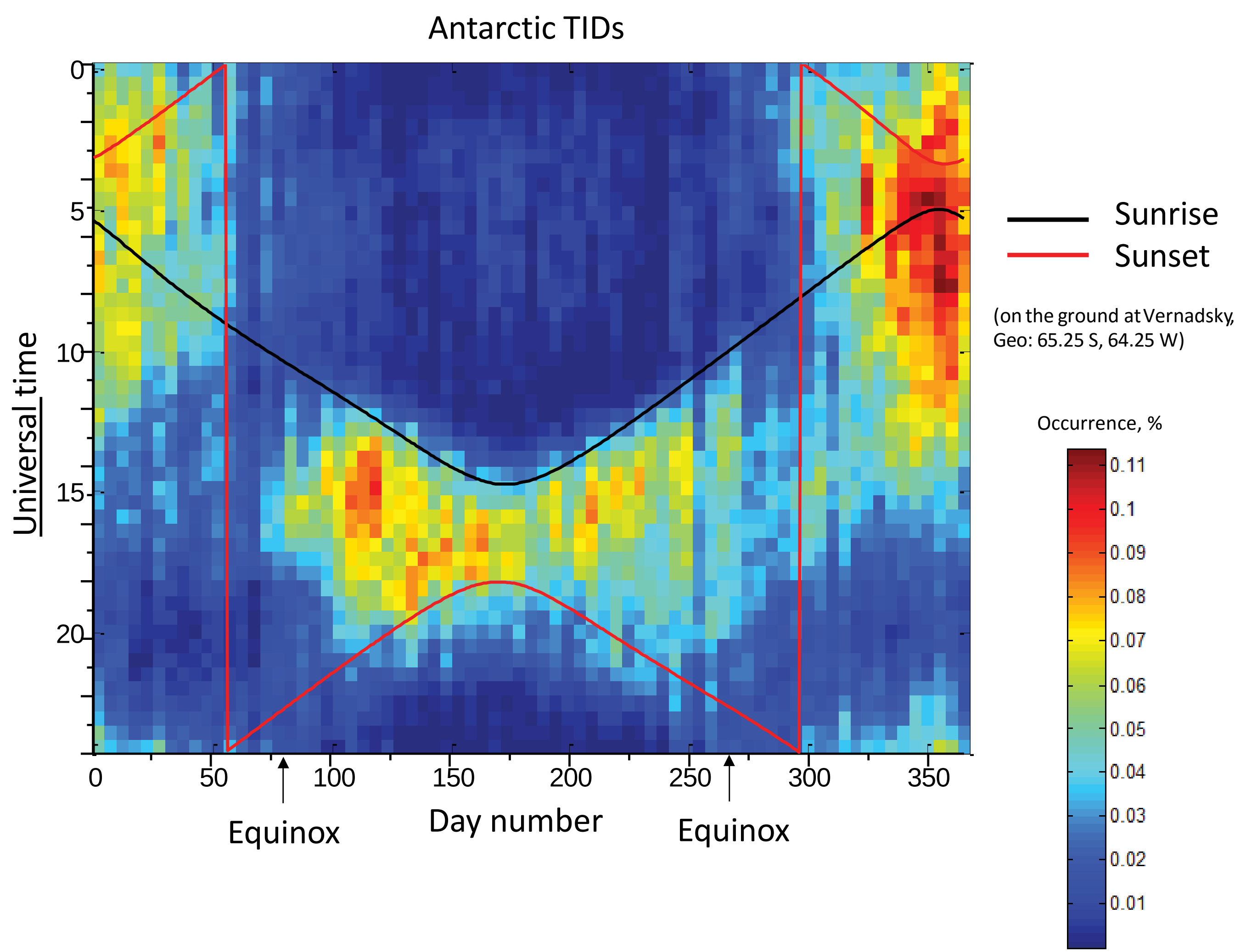

Strong correlation between TID occurrence and the solar terminator. In the mid-year (winter) TIDs are present only during the daytime and are apparently generated by the solar terminator passage over the observation point. During the other half of the year, TIDs are present most of the time, with the exception of the period around 20 UT (~16 LT) when a minimum in peak electron density is observed at that location. Apparently, during that time, there is not enough plasma to support TIDs.

Background plasma density distribution

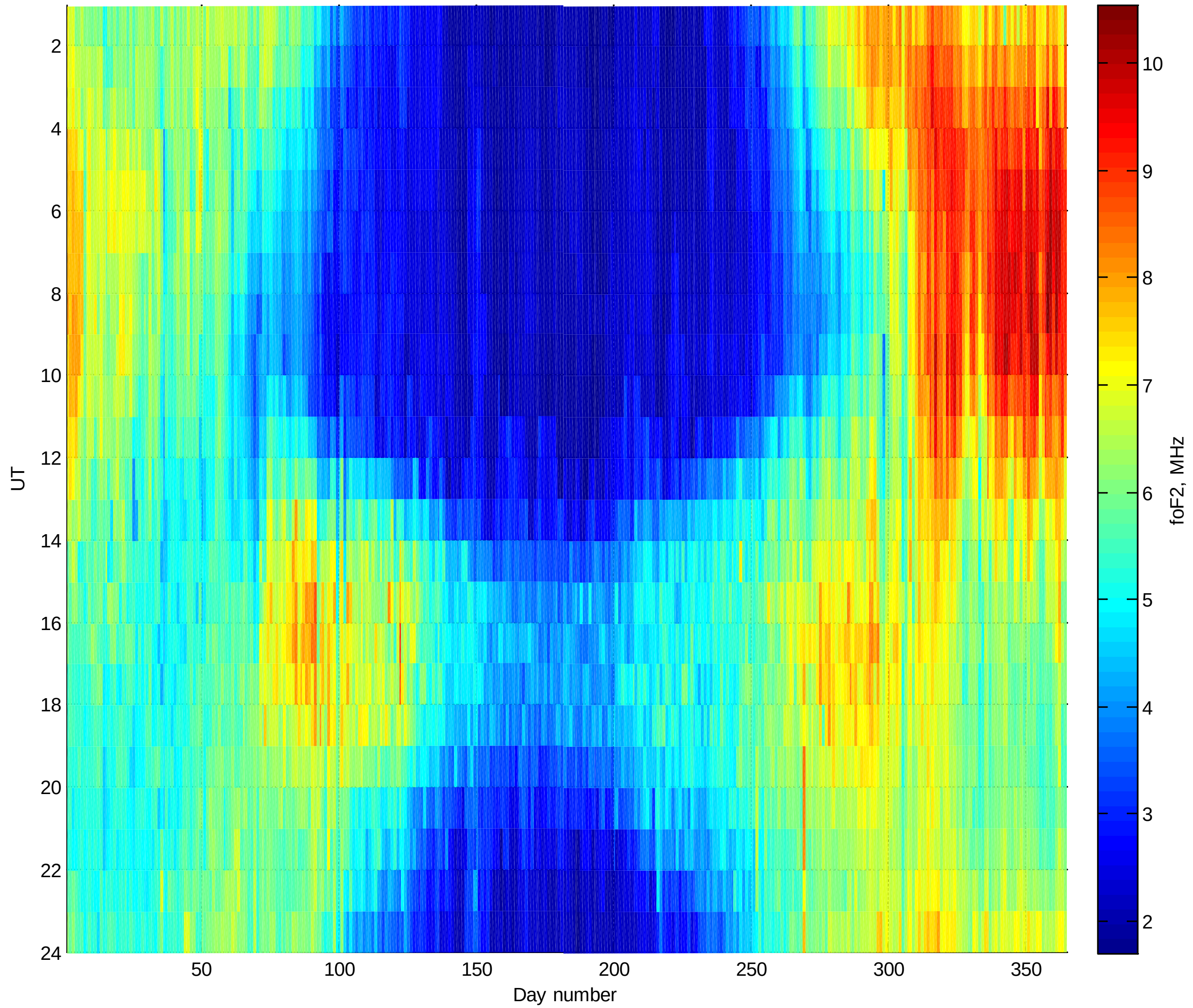

Measurements taken from Vernadsky ionosonde for years 2010-2011. Plasma density distribution is shown by critical frequency, foF2.

Are these TIDs?

Changes in virtual height... due to ...progression of a wave motion of such nature as to cause changes in ion concentration (for example, a pressure wave). [Munro, 1948]

..the reason for the repetition of small changes in region F2 ..a rapid east-west motion of or within region F2 ionization...[Beynon, 1948]

Quasi-periodic variations in the ionosphere: [e.g. *Ogawa et. al.*, 1987]
Period: 15-90 min
Velocity: 100-250 m/s
Horizontal wavelength: 100-1000km

Origin: AGWs [Hooke, 1968] or F region instability [Perkins, 1973].

How sensitive are TEC measurements, especially during the night time?

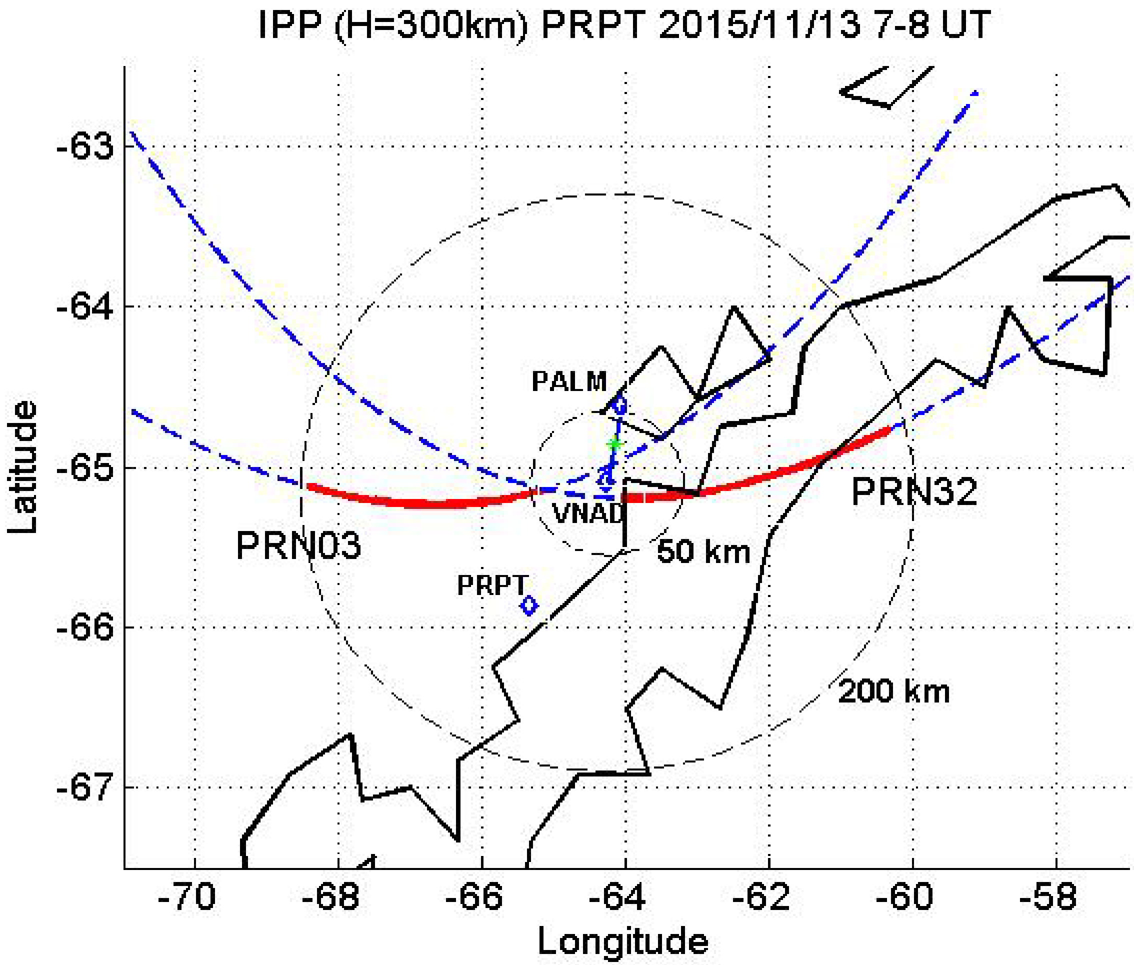

HF three-channel system diagram

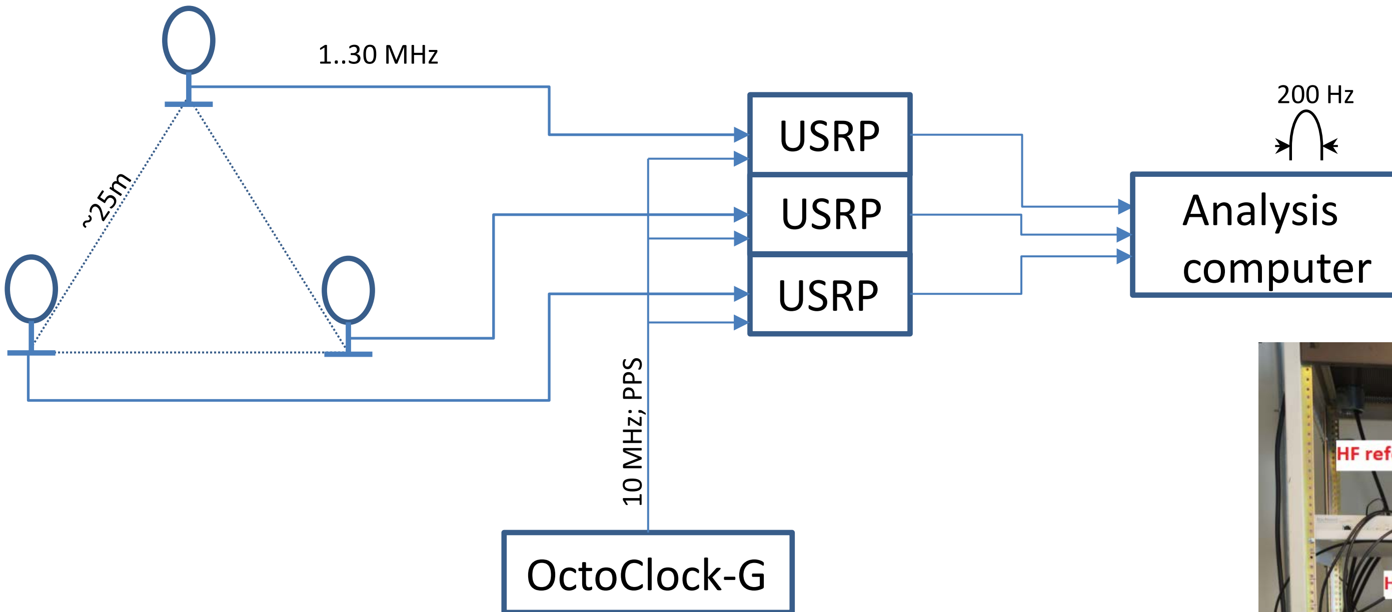

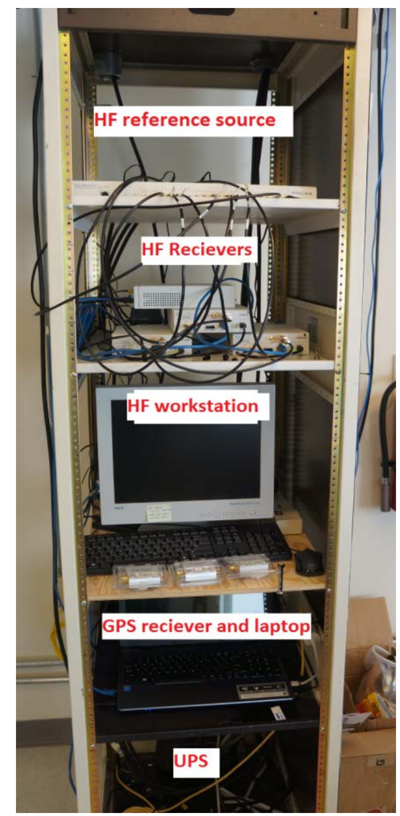

- **Built and installed three-channel HF receive system to measure AoA and Doppler**
- **Also installed Septentrio GNSS receiver**
- **Raw data shipped by sea, first significant data delivery made in January 2016**

USRP 210

HF 3-channel system antenna array

Left: three antenna array installed at Palmer station.

Distance between the antenna pairs is approximately 25 meters, and antennas are leveled to 1-2 cm accuracy.

Right: Antenna #2 close-up photo and curious native.

Example of very close match between HF and GNSS observations

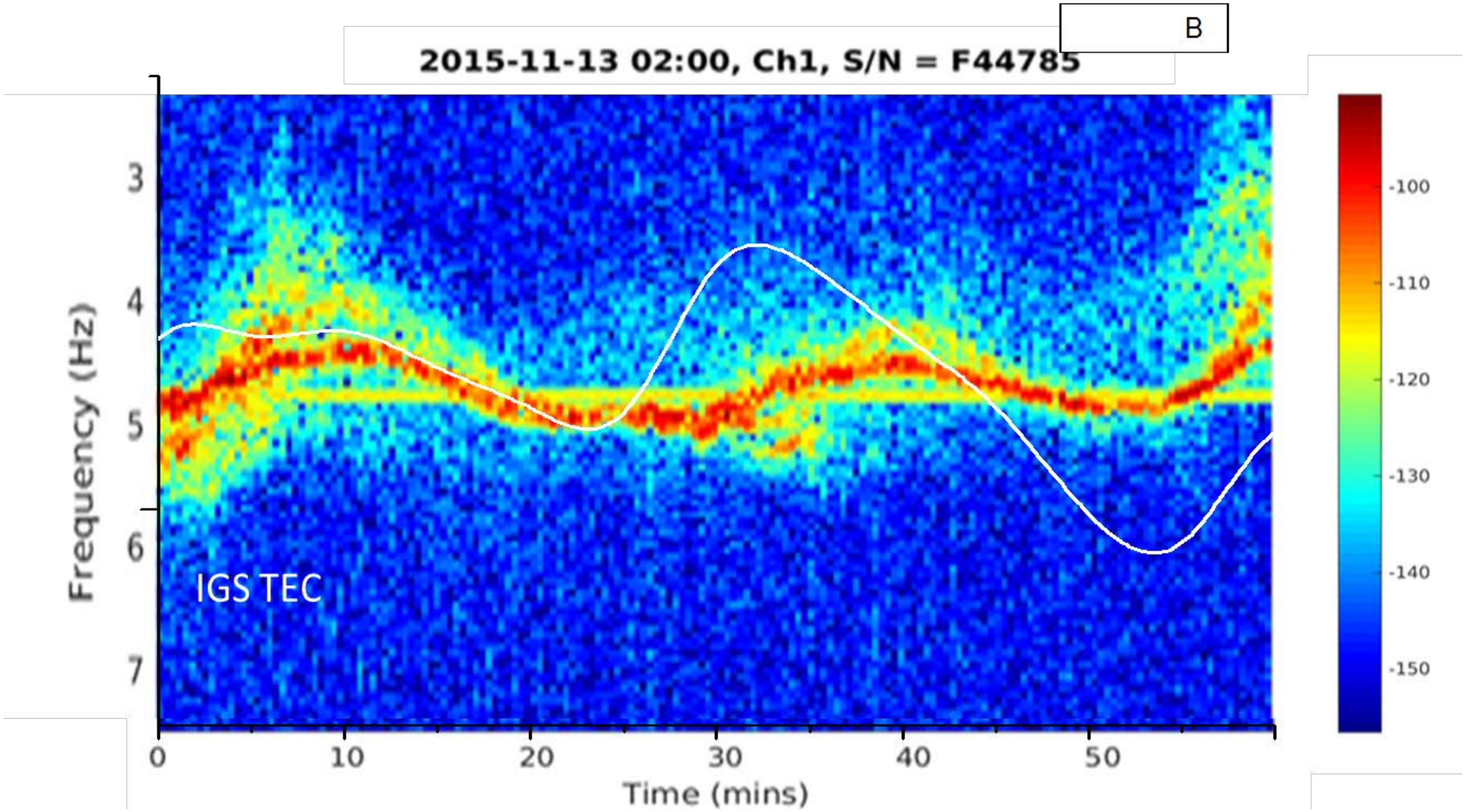

Nighttime observations in 2015: 83 nights (July-September 05-08 UT)
Doppler variations, (though weak) were observed almost 20% of the time
Daytime: 85 days (12-17 UT), variations observed more than 80% of the time.

HF and GPS Data Comparison

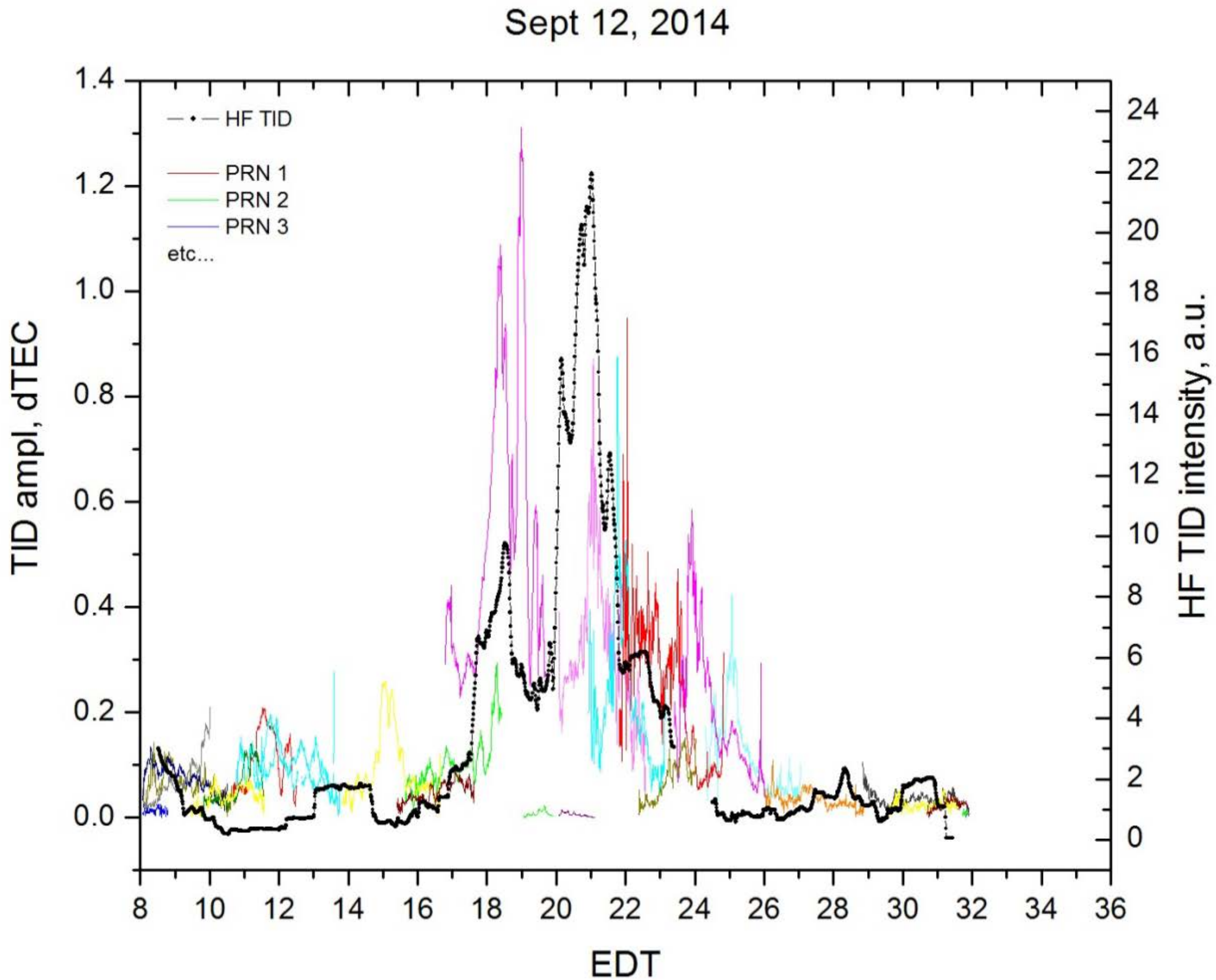

- Ratio of responses on GPS and HF varies significantly
- Note large GPS signature at 19:00 corresponds to relatively modest signature on HF; conversely, at 21:00 HF response exceeds GPS

Summary of TEC observations

- Using the dynamic interferometric approach to distrubance diagnostics from the GPS TEC measurements, a statistical picture of the TID occurrence over Antarctic Peninsula is established.

- Several disturbance modes have been shown to be present simultaneously: one with changing TID direction azimuth and at least two others with constant azimuthal directions of about -50 deg and 150 deg. The mode with changing azimuth is associated with the quiet time periods (Kp < 3) and is characterized by the TID propagation against the neutral wind.

- The anti-windward propagation is most likely associated with a wind shear filtering in the neutral atmosphere.

- TID climatology varies significantly during the year. During the winter mid-year the TID occurrence is controlled by the Solar Terminator, and the disturbances are present only during the day time. During the summer part of the year, disturbances are present for the most part of the day and are absent near 16 LT (minimum of in the local plasma density).
- The exact mechanism for the such pattern and the role of the Solar Terminator needs further investigation, but it is clear that the plasma density is a very important factor for the TID presence.

Questions

- How unique is this Antarctic pattern?
- Are these true TIDs observed?

Thanks for your attention!

Effect of electron density

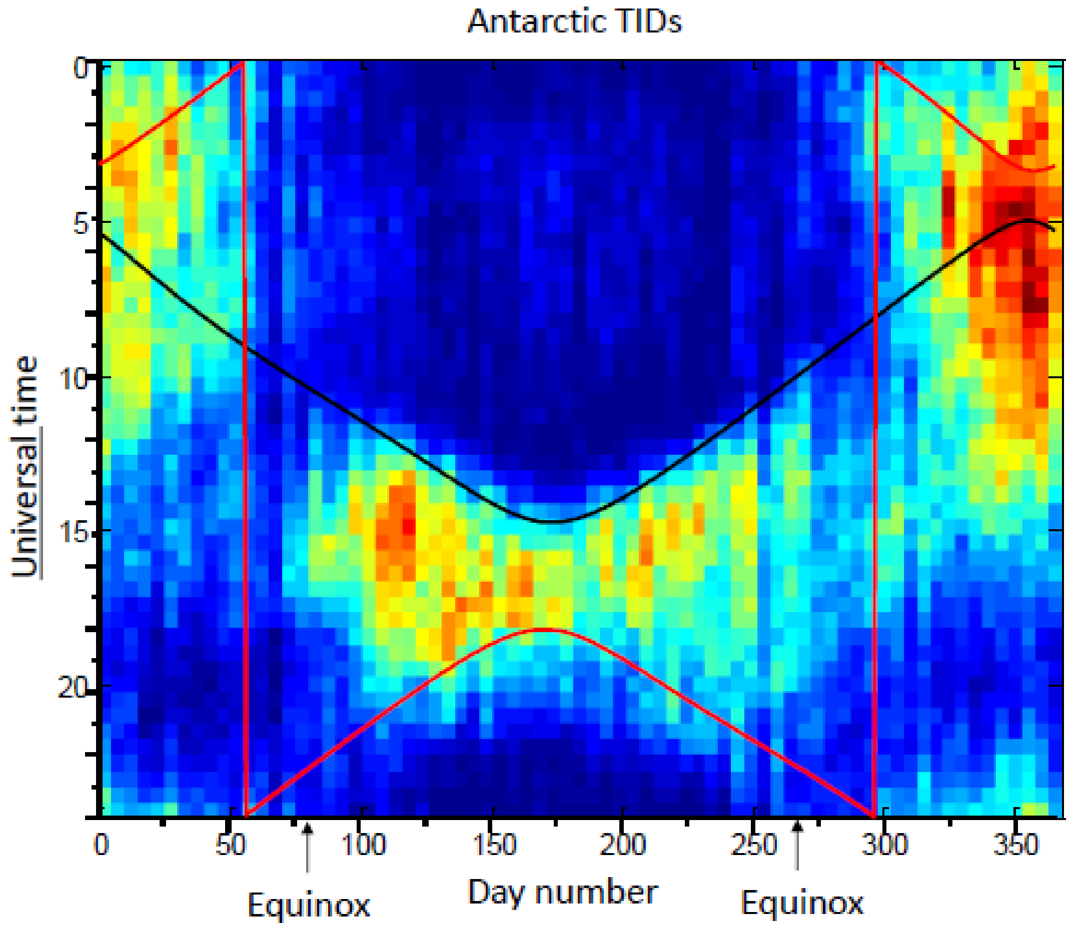

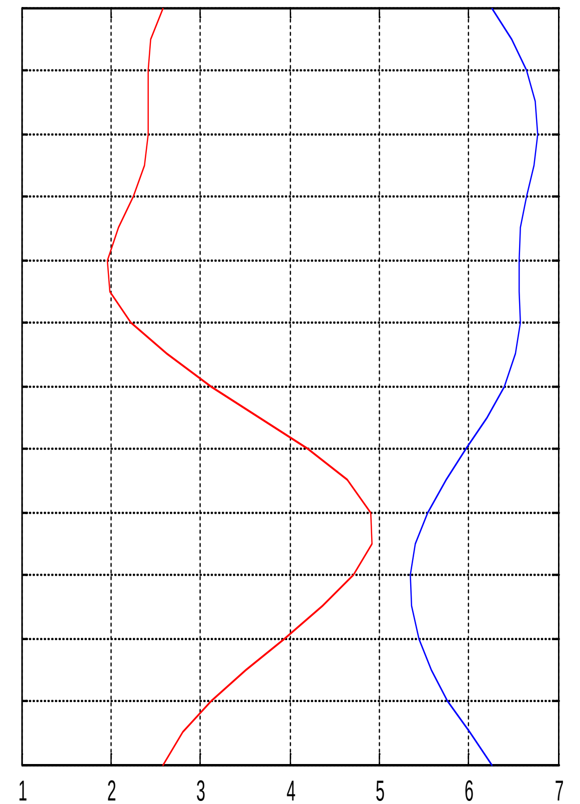

foF2 (MHz)
August 13, 2011
and
December 21, 2011

Absolut (calibrated) TEC is needed!

HF Frequency Angular Sounding (FAS) approach

- *Use bistatic (or vertical) HF measurements of trajectory signal parameter variations (AoA+Doppler) to determine TID parameters*

- Advantages:

  Cheap, simple, transmitters of opportunity can be used
- Disadvantages:

Essentially a single-point measurement; inversion of spatial TID parameters requires simplified TID model; high accuracy of AoA and Doppler required.

Digisonde observations of TIDs with frequency and angular sounding technique, Paznukhov, V. V.; Galushko, V. G.; Reinisch, B. W., 2012, Advances in Space Research, Volume 49, Issue 4, p. 700-710.

FAS model (mirror reflection)

$$H(\mathbf{r},t) = H_0[1 + h(x,y,t)]$$

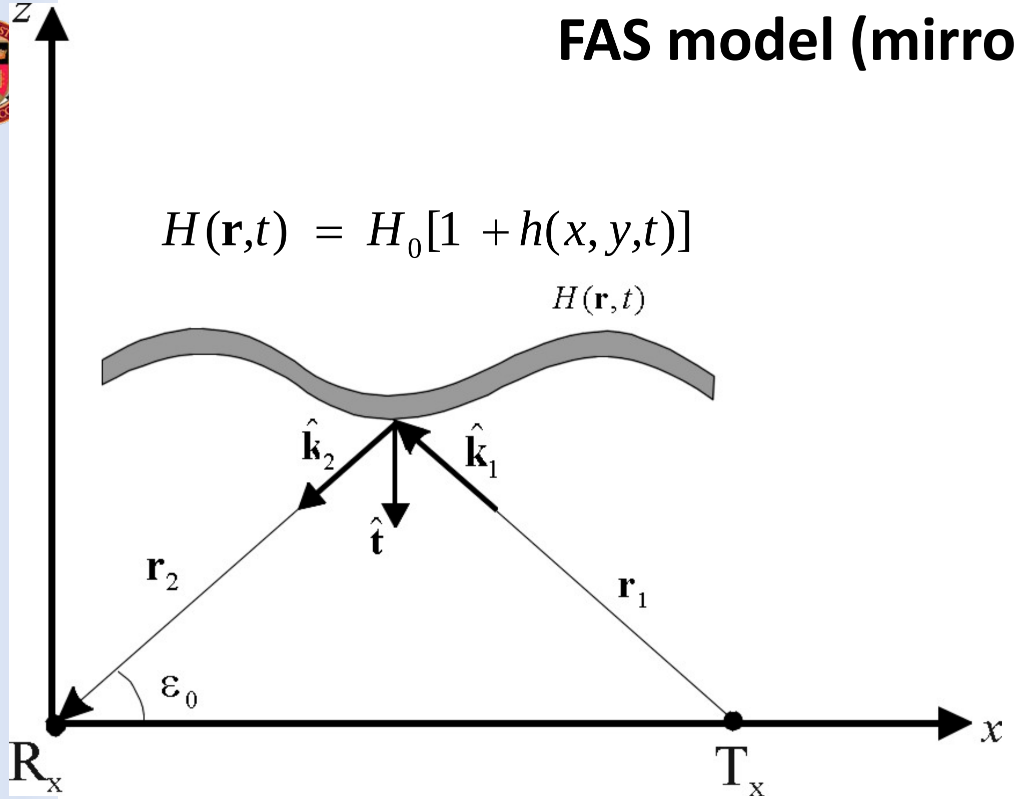

Perfectly reflecting surface model

Surface spectral representation:

$$h(x,y,t) = \int_{-\infty}^{\infty} N(\Omega) e^{i\Omega t} d\Omega e^{-iK(\Omega)(x\cos\theta(\Omega) + y\sin\theta(\Omega))}$$

$N(\Omega)$ – TID amplitude

$K(\Omega)$ – TID wavenumber

$\theta(\Omega)$ – TID direction of motion

Measured signal parameters:

ε(t) elevation angle

φ(t) azimuthal angle

f_D(t) Doppler shift

Spectral representations:

$$\varepsilon(t) = \int_{-\infty}^{\infty} S_\varepsilon(\Omega) e^{i\Omega t} d\Omega$$

$$\varphi(t) = \int_{-\infty}^{\infty} S_\varphi(\Omega) e^{i\Omega t} d\Omega$$

$$f_D(t) = \int_{-\infty}^{\infty} S_F(\Omega) e^{i\Omega t} d\Omega$$

$$\boxed{\varepsilon(t), \varphi(t), f_D(t) \Leftrightarrow h(x,y,t)}$$

(Beley et al., 1995; Paznukhov, 2004)

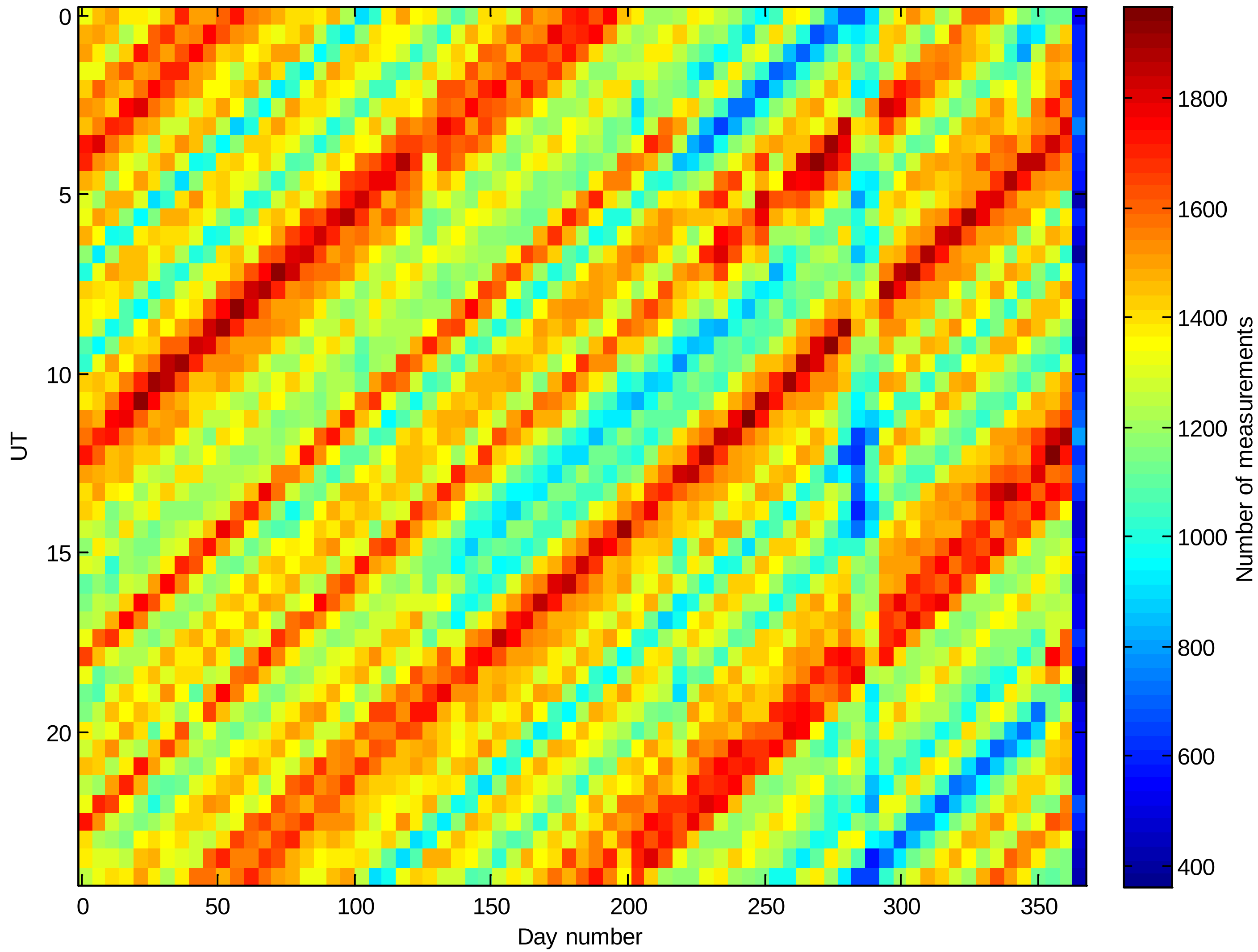

0
5
10
15
20
UT
0
50
100
150
200
250
300
350
Day number
1800
1600
1400
1200
1000
800
600
400
Number of measurements

FAS solution

With the use of the spectral representation, one gets solutions

Trajectory parameters spectra: (AoA and Doppler)

$$S_\varepsilon(\Omega) = N(\Omega)[\sin\varepsilon_0 \cos\varepsilon_0 - iH_0 K(\Omega)\cos\theta(\Omega)]$$
$$S_\varphi(\Omega) = iH_0 K(\Omega) N(\Omega)\tan\varepsilon_0 \sin\theta(\Omega)$$
$$S_F(\Omega) = -2iH_0 \Omega N(\Omega)\sin\varepsilon_0 / \lambda$$

Ratios between complex and real parts allow testing a hypothesis of a presence of idealized TID in the data

Reflecting surface spectra: (TID parameters)

$$N(\Omega) = \frac{i\lambda S_F(\Omega)}{2H_0\Omega \sin\varepsilon_0}$$

$$\tan\theta(\Omega) = -\frac{2H_0\Omega \operatorname{Re} S_\varphi(\Omega)}{2H_0\Omega \operatorname{Re} S_\varepsilon(\Omega)\tan\varepsilon_0 + \lambda \operatorname{Im} S_F(\Omega)\sin\varepsilon_0}$$

$$K(\Omega) = -\frac{2\Omega \operatorname{Im} S_\varphi(\Omega)\cos\varepsilon_0}{\lambda \operatorname{Im} S_F(\Omega)\sin\theta(\Omega)}$$

ICOM based transmitter (Vernadsky)

Transmitter assembly at Vernadsky station. The system includes ICOM-718 transceiver, antenna tuner, power supply box, modulator, and PC computer. Operational power ~10 W.

(Lives in the “Beastie’s” room)

First HF data from bistatic sounder

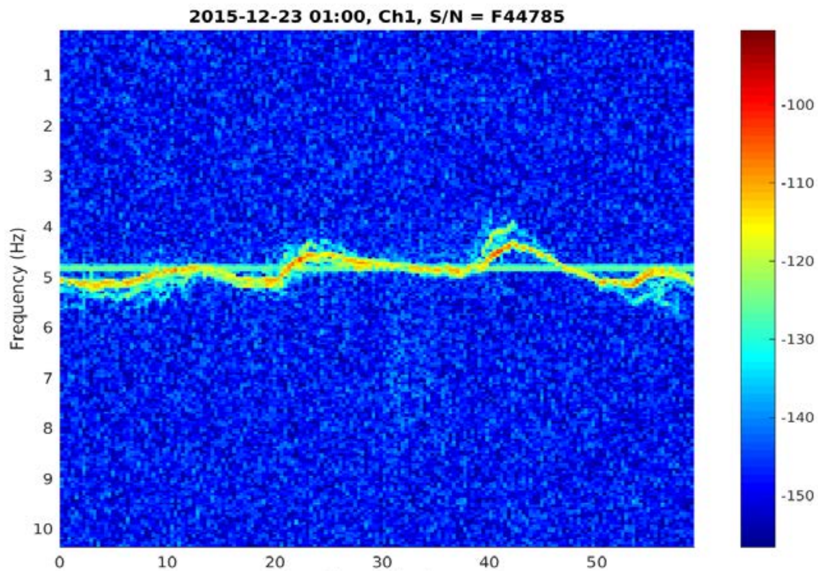

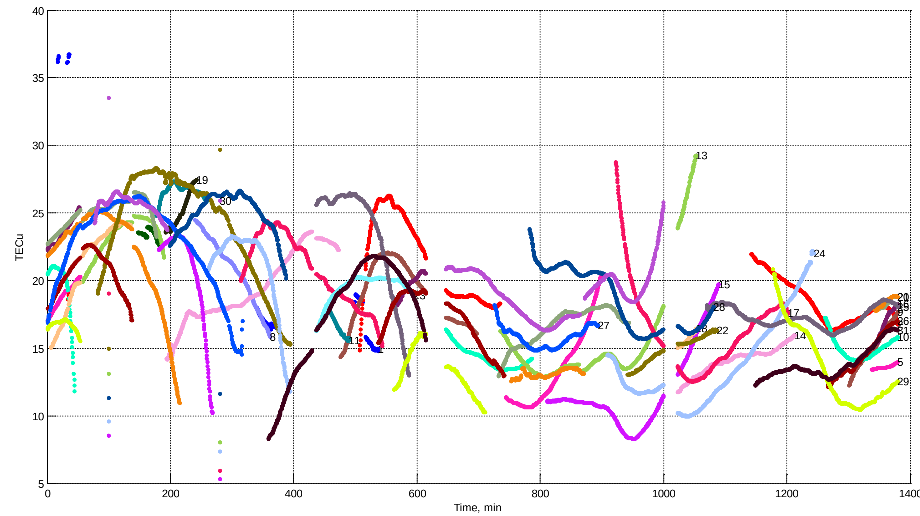

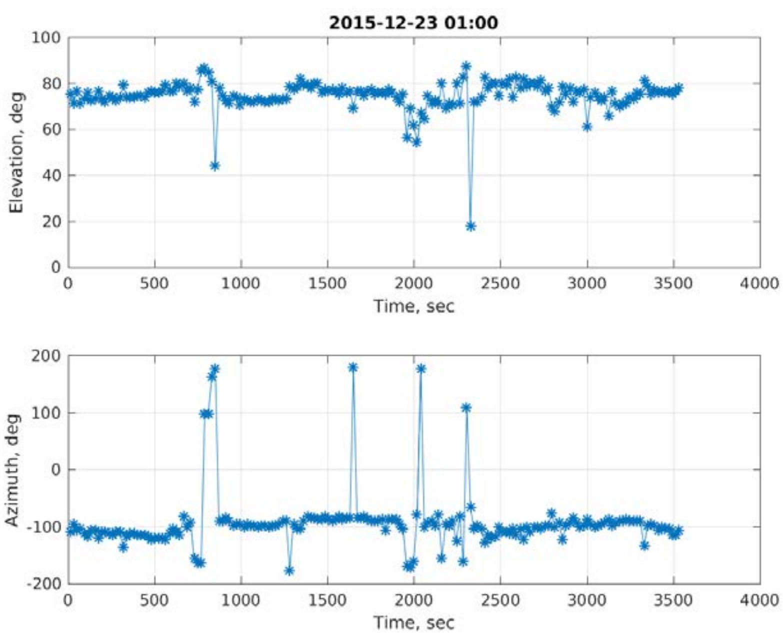

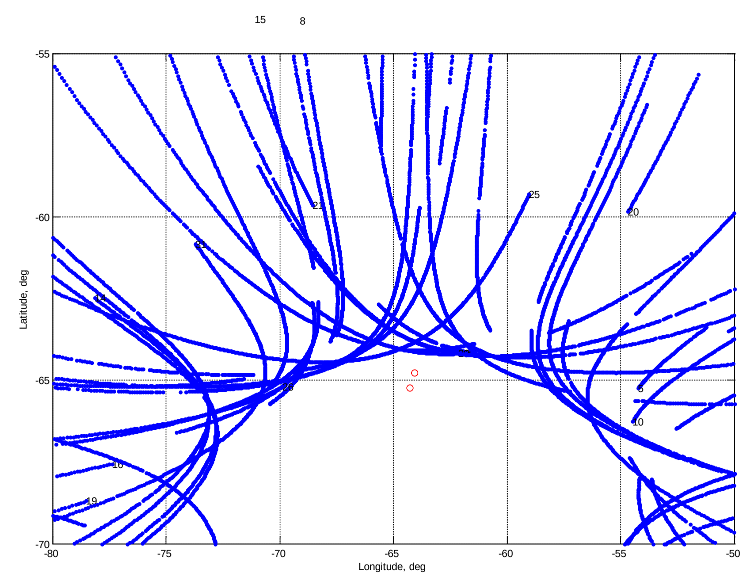

Simultaneous observations at two locations

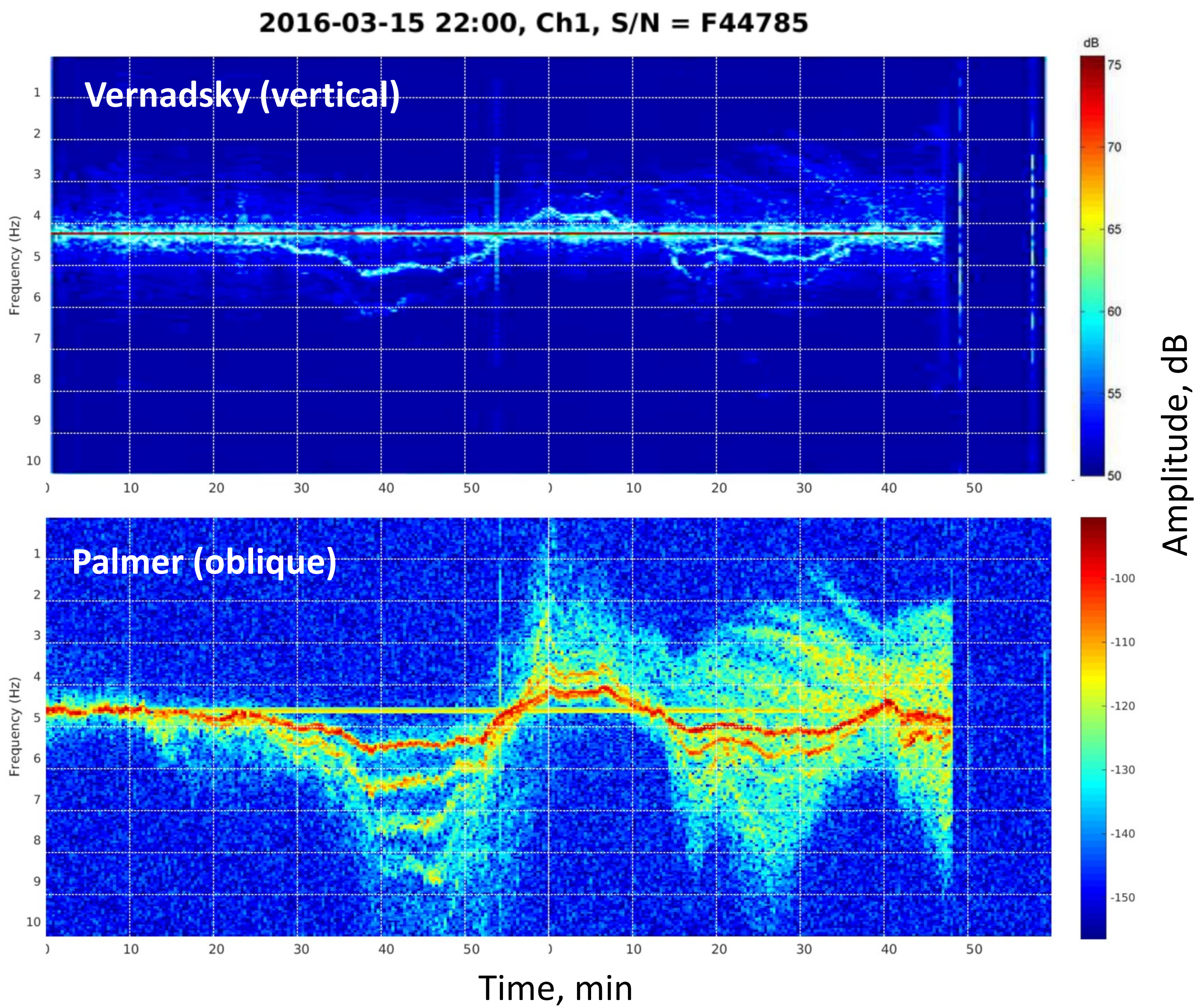

Summary

- Climatology of ionospheric disturbances in Antrarctic Peninsula region is controlled by neutral wind and solar terminator

- TEC observations provide an excellent tool for AGW/TIDs studies.

- HF observations of the bottomside ionosphere will help revealing details of TID generations and propagations and their relationship with the AGWs and tropospheric processes in general.

- How unique is this Antarctic pattern?

USRP N210 system

Research™
onal Instruments Company

USRP™ N200/N210 NETWORKED SERIES

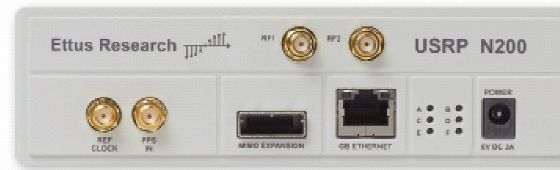

FEATURES:

- Use with GNU Radio, LabVIEW™ and Simulink™
- Modular Architecture: DC-6 GHz
- Dual 100 MS/s, 14-bit ADC
- Dual 400 MS/s, 16-bit DAC
- DDC/DUC with 25 mHz Resolution
- Up to 50 MS/s Gigabit Ethernet Streaming
- Fully-Coherent MIMO Capability
- Gigabit Ethernet Interface to Host
- 2 Gbps Expansion Interface
- Spartan 3A-DSP 1800 FPGA (N200)
- Spartan 3A-DSP 3400 FPGA (N210)
- 1 MB High-Speed SRAM
- Auxiliary Analog and Digital I/O
- 2.5 ppm TCXO Frequency Reference
- 0.01 ppm w/ GPSDO Option

N200/N210 PRODUCT OVERVIEW:

The Ettus Research™ USRP™ N200 and N210 are the highest performing class of hardware of the USRP™ (Universal Software Radio Peripheral) family of products, which enables engineers to rapidly design and implement powerful, flexible software radio systems. The N200 and N210 hardware is ideally suited for applications requiring high RF performance and great bandwidth. Such applications include physical layer prototyping, dynamic spectrum access and cognitive radio, spectrum monitoring, record and playback, and even networked sensor deployment.

The Networked Series products offers MIMO capability with high bandwidth and dynamic range. The Gigabit Ethernet interface serves as the connection between the N200/N210 and the host computer. This enables the user to realize 50 MS/s of real-time bandwidth in the receive and transmit directions, simultaneously (full duplex).

USRP N210 System Specification

SPECIFICATIONS

Spec	Typ.	Unit
POWER		
DC Input	6	V
Current Consumption	1.3	A
w/ WBX Daughterboard	2.3	A
CONVERSION PERFORMANCE AND CLOCKS		
ADC Sample Rate	100	MS/s
ADC Resolution	14	bits
ADC Wideband SFDR	88	dBc
DAC Sample Rate	400	MS/s
DAC Resolution	16	bits
DAC Wideband SFDR	80	dBc
Host Sample Rate (8b/16b)	50/25	MS/s
Frequency Accuracy	2.5	ppm
w/ GPSDO Reference	0.01	ppm

Spec	Typ.	Unit
RF PERFORMANCE (W/ WBX)		
SSB/LO Suppression	35/50	dBc
Phase Noise (1.8 Ghz)		
10 kHz	-80	dBc/Hz
100 kHz	-100	dBc/Hz
1 MHz	-137	dBc/Hz
Power Output	15	dBm
IIP3	0	dBm
Receive Noise Figure	5	dB
PHYSICAL		
Operating Temperature	0 to 55°	C
Dimensions (l x w x h)	22 x 16 x 5	cm
Weight	1.2	kg

USRP N210 System Diagram

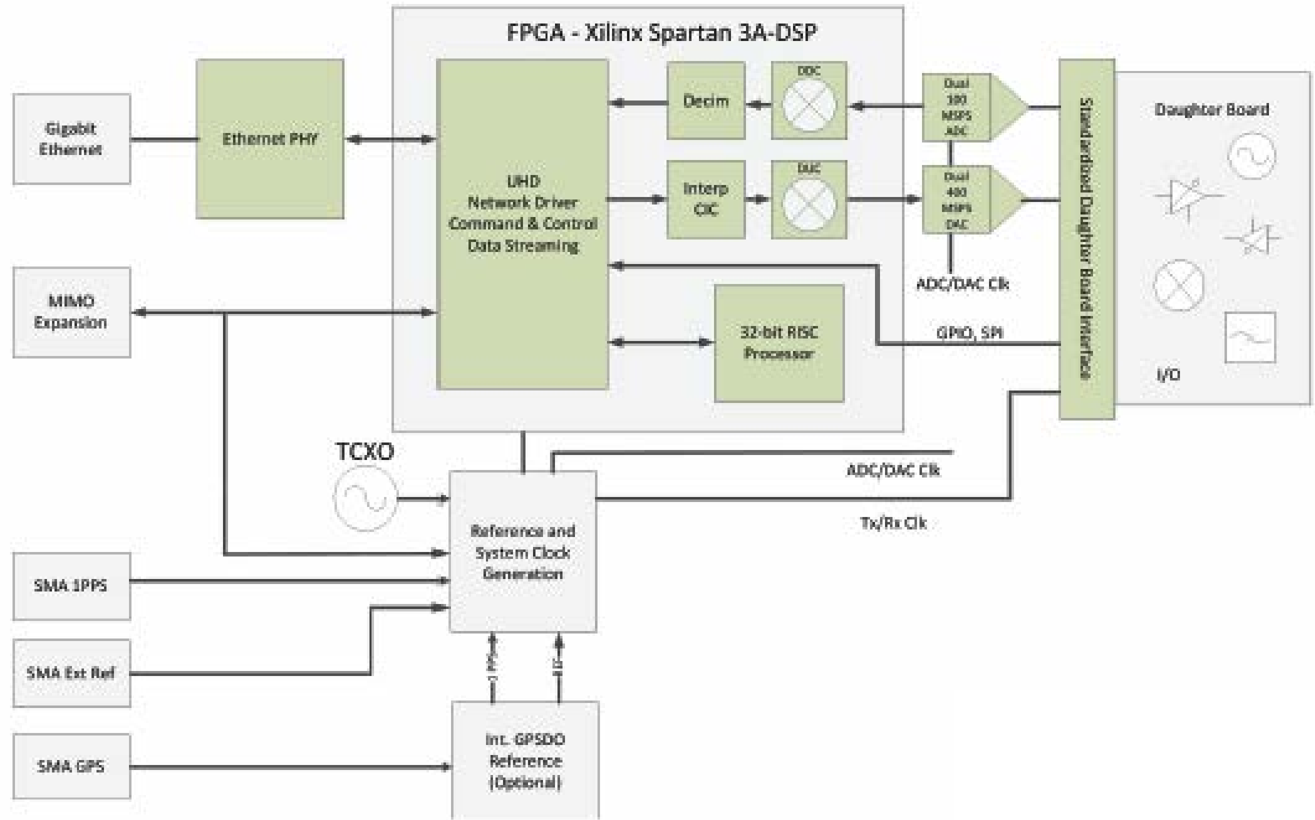

Daughtercard provides a frontend to the system.
FPGA provides downconversion, decimation, and filtering
The data is streamed through Gigabit Ethernet.